Techniques for the Design of Active Flow Control Systems in Heavy Vehicles

David E. Manosalvas[*], Thomas D. Economon[†], and Antony Jameson[‡]

Stanford University, Stanford, CA, 94305, USA

Francisco D. Palacios[§]

The Boeing Company, Long Beach, CA, 90808, USA

This article focuses on the computational study of active flow control systems, such as Coanda jets, and the effects that these have on the drag and power consumption of heavy vehicles. To simulate the flow over the Ground Transportation System (GTS) model, which is a simplified geometrical model used to represent heavy vehicles, the second order Unsteady Reynolds-Averaged-Navier-Stokes (URANS) equations were used. A top-view two-dimensional representation of the GTS model has been used to perform this study, and by adding Coanda jets to the trailing end, we aim to understand the aerodynamic effects of modifying the Coanda surface geometry, as well as the Coanda jet strength. Leveraging on the shape deformation capabilities integrated into SU2, an open source Computational Fluid Dynamics (CFD) suite, the shape of the Coanda surface has been controlled while the jet strength has been imposed by varying the plenum pressure. Computational simulations of the described geometry were used to generate a surrogate model of the power required by the vehicle. Finally, the surrogate model was used to visualize the design space, find trends, and understand the effect that the Coanda jets have on vehicle aerodynamics and energy consumption.

I.   Introduction and Motivation

It is well known that the potential for fuel, energy, and cost savings in US ground transportation is huge: just a 12% reduction in fuel use across the national fleet of heavy vehicles would save 3.2 billion gallons of diesel per year and prevent 28 million tons of CO_2 emissions.[1] Heavy vehicles, such as large freight transport trucks and trailers, account for 12-13% of all US petroleum consumption.[1] Due to their heavy usage and standard configuration, these vehicles are the perfect target for aerodynamics studies focused on drag reduction.

The aerodynamics of heavy vehicles are mainly characterized by flow separation and the development of low pressure turbulent wakes.[2] While great aerodynamic improvements have been made on the tractor with the use of passive techniques, there is still room for improvement in the trailer which is responsible for 50-60% of the total drag.[3] The majority of drag generated by the trailer is caused by the development of a low pressure wake, which causes a higher resistance to motion and is called viscous pressure drag or base drag. Aside from basic streamlining, viscous pressure drag can be reduced by the use of active flow control techniques.[4] Active flow control systems reduce the amount of separation which increases the pressure inside the wake and reduces the overall vehicle drag. Wind tunnel experiments using Coanda jets positioned on the trailing end of a trailer have shown that this type of active flow control system is capable of keeping the flow attached longer and increasing the wake pressure.[4] These experiments have demonstrated not only drag reduction, resulting in a net power savings of more than 15%, but also an improvement in vehicle stability and safety. The latter has been achieved by compensating for the effect of side forces by independently controlling each flow actuator.[2]

---

[*]Ph.D. Candidate, Department of Aeronautics & Astronautics, AIAA Student Member.
[†]Postdoctoral Scholar, Department of Aeronautics & Astronautics, AIAA Senior Member.
[‡]Research Professor, Department of Aeronautics & Astronautics, AIAA Fellow.
[§]Engineer, Advanced Concepts Group, AIAA Senior Member.

American Institute of Aeronautics and Astronautics

For the effective design of active flow control systems, it is necessary to understand the effects that each part of the system has on the flow features. To approach the design process using Computational Fluid Dynamics (CFD), the numerical schemes and turbulence models have to be carefully selected to preserve accuracy on a limited computational budget. The problem in hand requires the computation of the integrated forces over the Ground Transportation System (GTS) model, for which it is particularly important to simulate the unsteady flow behavior, vortex shedding frequency, and to obtain an accurate prediction of boundary layer separation.

Due to the complexity of the problem, Large Eddy Simulation (LES) is believed to be the most reliable method when it comes to the prediction of flow features and integrated forces in separated flows. Unfortunately, this approach increases the computational requirements significantly, making it prohibitively expensive for its use through the design process. In order to be able to use CFD for the design of active flow control systems, it is necessary to use a combination of tools that will allow us to simulate the flow around the GTS model with an acceptable level of accuracy. A study of this problem was published by the authors in 2014,[5] and the computational tools found to agree the closest to the experimental data available will be used for this study.

The purpose of this article is to better understand the aerodynamic variations caused by the Coanda surface geometry and the jet strength. Guided by a surrogate model of the power coefficient, the effect that these variables have in the flow structure, aerodynamic performance and power consumption of the vehicle is explained. To fulfill this objective the paper is laid out as follows. In Section II, a description of the geometry used for the simulation of the flow around the GTS model and the flow conditions are presented. Section III, introduces the numerical scheme and turbulence model combination that has been used, presents the computational grids, a description of the boundary conditions, introduces the variables that have been used to explore the design space and the methods to control them, as well as a description of the method used to generate the surrogate model. In Section IV, the prevalent flow features at different Coanda jet configurations have been analyzed and the trends exposed by the surrogate model are described. Finally, Section V, summarizes the results and introduces suggestions for future work.

II.   Physical Model

To focus on the study of the aerodynamic features that characterize separated flows, and the influence that active flow control has on the presence of viscous pressure drag, a clean model of a heavy vehicle is required.[3] Heavy vehicles have a variety of features that contribute towards flow separation, such as mirrors, antennas, gaps, mud flaps, etc. and to eliminate the effect that these have, the GTS model was used. The GTS model removes all the detailed features including the tractor-trailer gap, and the height difference. This geometrical model effectively combines both the tractor and the trailer into a single simplified bluff body that has a semicircular leading shape and ends in a sharp straight cut in the back. A 6.5% scale GTS model, similar to the one used by Englar,[4,6] was used for this analysis.
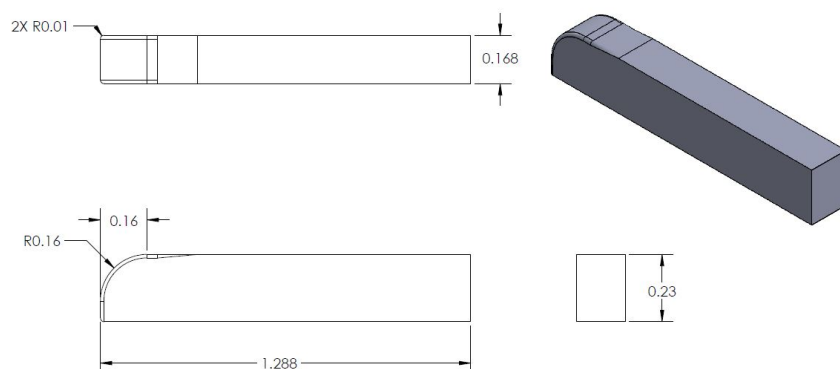

Figure 1. Baseline three-dimensional GTS model - Scale 0.065. All dimensions in meters.

In addition to the base model in Figure 1, a model which includes Coanda jets in all four corners of the

American Institute of Aeronautics and Astronautics

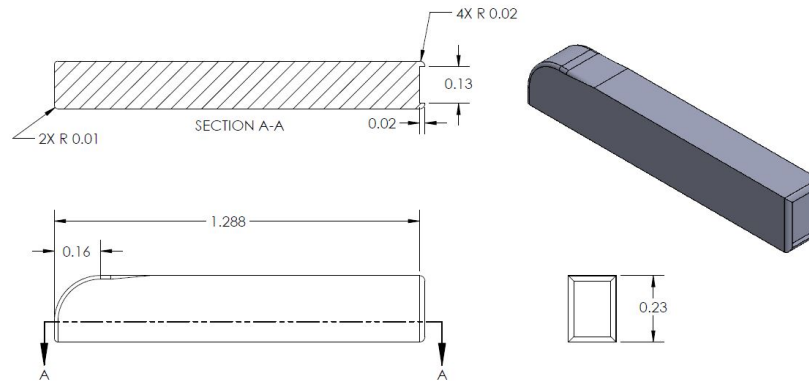trailing edge was generated and is shown in Figure 2.

Figure 2. Three-dimensional GTS model with Coanda Jets in the trailing edge - Scale 0.065. All dimensions in meters.

To reduce the computational costs of exploring the effects of manipulating the Coanda surface geometry and jet blowing strength, a two-dimensional model capable of representing the prominent flow features was selected. The principal effects of active flow control that this study aims to analyze are drag reduction, which leads to reduced power consumption, as well as lateral stability which is a consequence of vortex shedding reduction. For this purpose, the top-view of the GTS model was chosen. The two-dimensional geometries are shown in Figure 3.
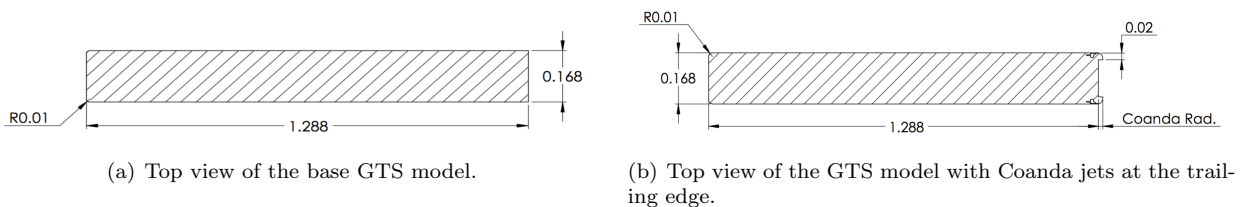

(a) Top view of the base GTS model.

(b) Top view of the GTS model with Coanda jets at the trailing edge.

Figure 3. Two-dimensional GTS models - Scale 0.065. All dimensions in meters.

Although the flow around a ground vehicle has a variety of three-dimensional effects, the two-dimensional top-view allowed us to study the effects of the boundary layer, flow separation, and vortex shedding on the drag of the vehicle, as well as the lateral forces induced by the unsteady wake.
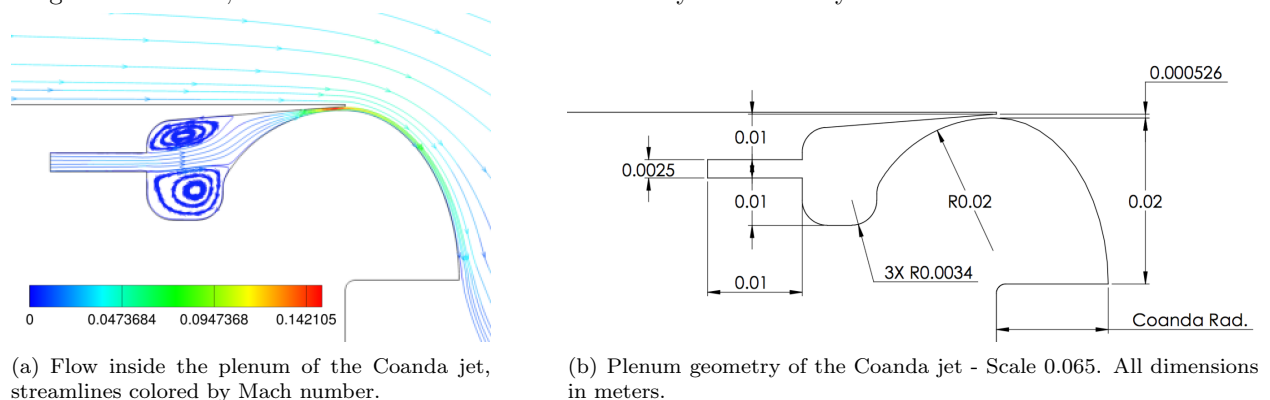

(a) Flow inside the plenum of the Coanda jet, streamlines colored by Mach number.

(b) Plenum geometry of the Coanda jet - Scale 0.065. All dimensions in meters.

Figure 4. Coanda jet model and flow features.

To simulate the jet flow injection, a plenum-jet interaction was included in the geometrical model. For this purpose, inspiration was taken from the Englar airfoil.[7] In general, the chosen plenum shape enhances the

American Institute of Aeronautics and Astronautics

strain behavior of the flow, which is achieved by generating two standing vortices that guide the flow towards the Coanda surface. The path taken by the flow, and its interaction with the internal vortices, reduce the wall effect and allows for a cleaner flow, which helps prevent premature boundary layer separation. Figure 4 shows the Coanda jet geometry and the described flow features.

The GTS model was analyzed using standard air threated as a calorically perfect ideal gas at standard temperature and pressure (STP) conditions. The velocity chosen to match the standard cruise speed was $31.3 \frac{m}{s}$ (70 mph) which translates to a Mach and the Reynolds numbers, as a function of the GTS model length (Lc), of 0.09195 and 2.759 million, respectively. The power required to overcome the aerodynamic drag is:

$$P_{aero} = D * U_\infty, \tag{1}$$

where D is the aerodynamic drag and U_∞ is the free stream velocity. The power required to energize each Coanda jet is the compressor power:

$$P_{comp} = \frac{\dot{m}_e * c_p * (T_f - T_i)}{\eta}, \tag{2}$$

which has been calculated using a thermodynamic compressor model. The mass flow rate through the jet is $\dot{m}_e$, c_p is the constant pressure specific heat, T_f is the plenum fluid temperature which was set to 477.594 K to maximize the jet momentum,[4,6] T_i is the fluid temperature before entering the compressor and η is the compressor's isentropic efficiency which has been set to 90%. To better characterize the strength of the jet, drag of the vehicle, power consumption, lateral forces and vortex shedding frequency; non-dimensional coefficients for these quantities have been defined as follows:

$$C_P = \frac{P_{aero} + 2 * P_{comp}}{q * U_\infty * W}, \qquad C_\mu = \frac{\dot{m}_e * V_e}{q * W}, \qquad C_D = \frac{D}{q * W}, \qquad C_{LF} = \frac{LF}{q * W}, \qquad St = \frac{f * W}{U_\infty}, \tag{3}$$

where C_P is the power coefficient, q is the dynamic pressure calculated as $\frac{1}{2}\rho_\infty U_\infty^2$, ρ_∞ is the free stream density, W is the width of the base GTS model, C_μ is the momentum coefficient, V_e is the flow velocity at the jet's exit, C_D is the drag coefficient, C_{LF} is the lateral force coefficient, LF is the lateral force, St is the Strouhal number and f is the vortex shedding frequency.

III.   Numerical Tools

A.   Computational Fluid Dynamics (CFD) Setup

To model the flow around the two-dimensional base and the enhanced GTS model, the SU2[8,9] compressible solver using the second-order Jameson-Schmidt-Turkel (JST)[10] numerical scheme combined with the Shear Stress Transport (SST)[11] turbulence model were chosen based on the study published by the authors in 2014.[5] The viscous terms were computed using the weighted least squares method and time accurate integration was achieved with a second order backward difference dual time stepping approach.[12] To better model the periodicity of the flow a physical time step of 500 μs was chosen, representing each period by using between 60 and 120 points depending on the shedding frequency. To maintain the required time integration accuracy, three orders of magnitude of pseudo-time convergence were used at each physical time step.
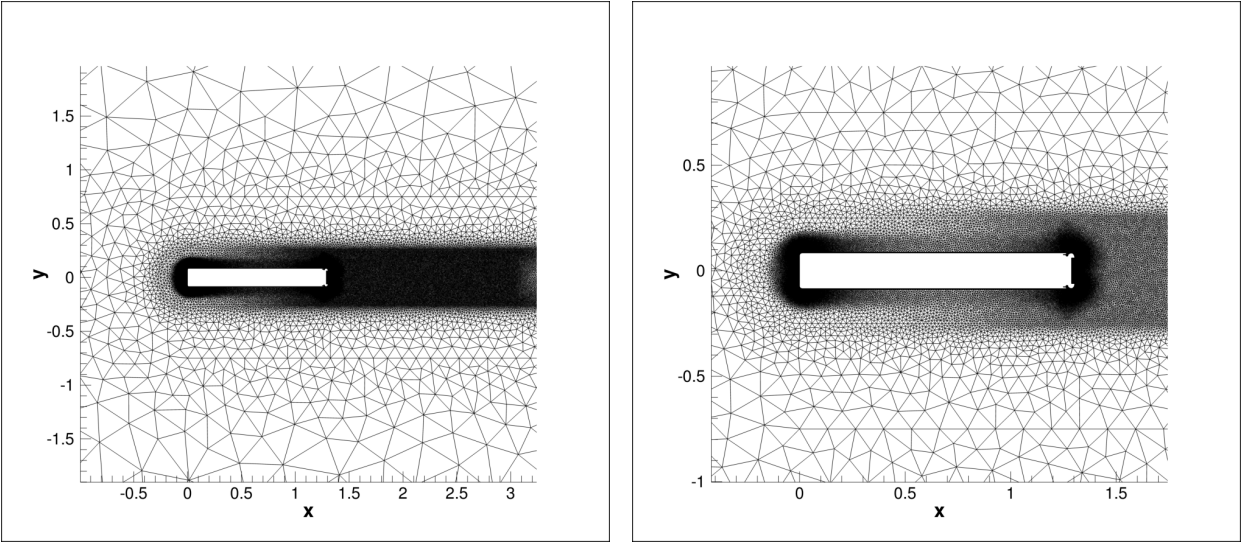
B.   Computational Mesh

The two-dimensional domains were discretized using a hybrid mesh, which consists of a structured mesh near the walls to better capture the boundary layer behavior, and an unstructured mesh towards the farfield, for a more aggressive growth rate while keeping a healthy aspect ratio of the elements. To properly resolve the boundary layer a $Y+$ of 0.8 was used. The meshes used, shown on Figures 5 and 6, are $15L_c$ in length and $11L_c$ in width, which in addition to the use of characteristic farfield boundary conditions, has been used to prevent pressure wave reflections. The mesh for the base GTS model has 88,275 cells and 52,915 points, and the mesh for the enhanced GTS model, which includes the Coanda jets at the trailing edge, has 140,259 cells and 89,572 points. The radical increase in mesh size is due to the addition of the jets and the resolution required to model the plenum. The mesh used to model the Coanda jets is shown in Figure 7.

American Institute of Aeronautics and Astronautics
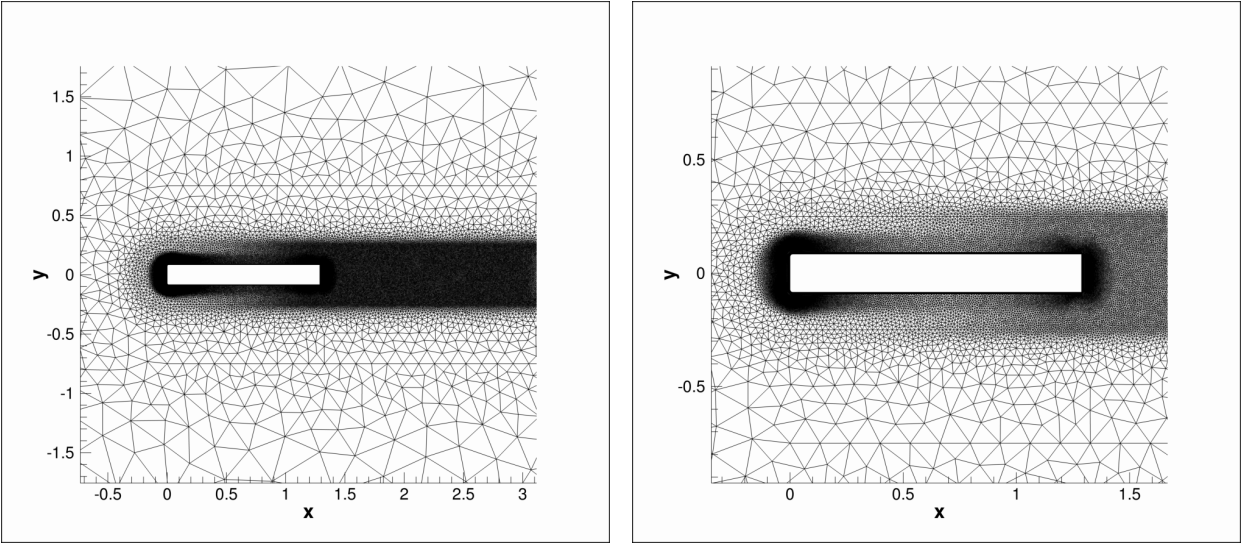
(a) Base GTS mesh including a wake refinement region.

(b) Base GTS mesh near-field.

Figure 5. Computational grid for the base GTS model.

(a) Enhanced GTS mesh including a wake refinement region.

(b) Enhanced GTS mesh near-field.

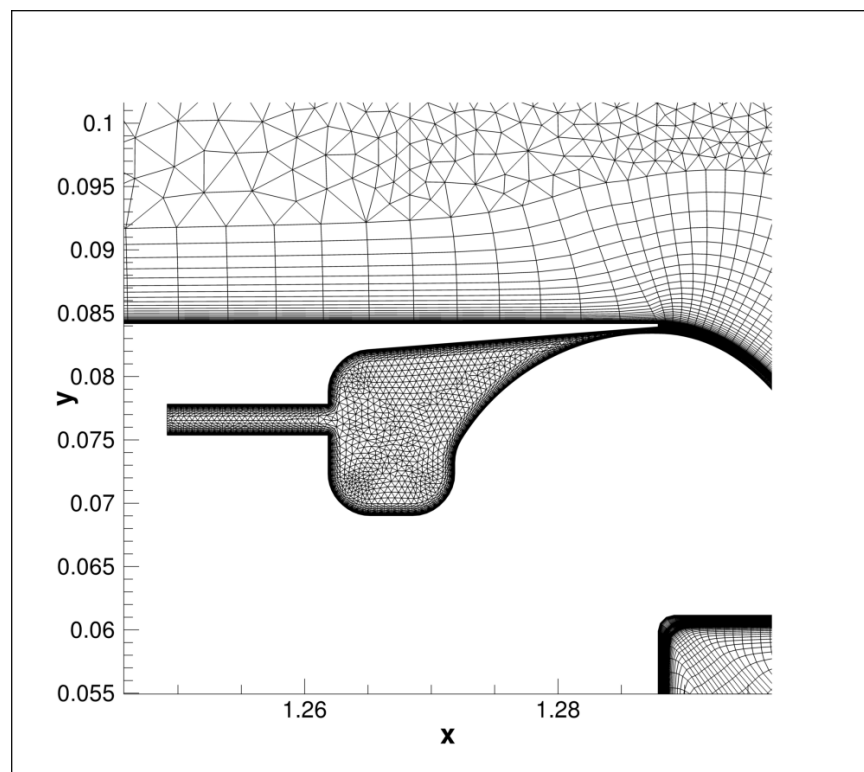**Figure 6. Computational grid for the enhanced GTS model.**

American Institute of Aeronautics and Astronautics

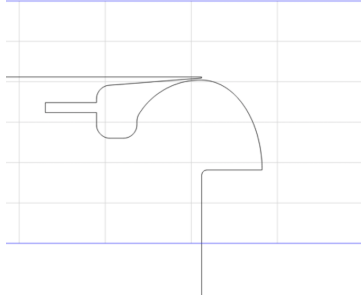**Figure 7. Computational grid used to model the Coanda jet.**

C. Design Space Exploration

To properly design active flow control systems capable of significantly reducing harmful gas emissions and vehicle energy consumption, it is important to understand the effects that jet injection strength and the Coanda surface geometry have on the overall vehicle aerodynamic behavior. Although the numerical approach taken for this study has significantly reduced the computational expense, the unsteady nature of the flow makes the use of parametric studies prohibitively expensive for design purposes. As such, we use a surrogate model to represent the power coefficient (C_P) as a function of the Coanda radius and the momentum coefficient (C_μ).

The momentum coefficient was bounded between 0.00 and 0.05, based on the work by Englar in 2001[4] and the previous work on this topic by the authors.[5] This variable was controlled by varying the plenum pressure between $101,325$ and $106,029 \ Pa$. The Coanda radius has been modified through the use of Free Form Deformation (FFD) boxes, and the Coanda radius constraints were determined by visual inspection of the surrounding mesh quality after deformation. This technique maintains the overall mesh count and distribution constant making it ideal for design studies. The selected values for the Coanda radius ranged from 0.01 to 0.0286 m, which were controlled by varying the rightmost side of the FFD box from 0.00 to 0.05. The Coanda radius variation and FFD boxes are shown in Figure 8.

The design space was sampled 14 times with the use of a Latin-Hypercube[13] and the results obtained from these simulations were used to compute the length scales and surface fitting coefficient required for the proper generation of the C_P surrogate using a Gaussian Process Regression (GPR).[13] To better match the expected behavior, the boundary values used to generate the C_P surrogate model were set to 0.82, which was determined based on the author's previous work[5] and verified by the simulations representing low momentum coefficient conditions. The GPR model and machine-learning toolbox used for this study were implemented by Lukaczyk[14] and can be found on a GitHub open source repository under the name of "VyPy" [a].

---

[a]https://github.com/aerialhedgehog/VyPy

American Institute of Aeronautics and Astronautics

(a) Original Coanda jet geometry and FFD bounding box with control points at the intersection of the gray lines. Coanda Radius is 0.01 m.
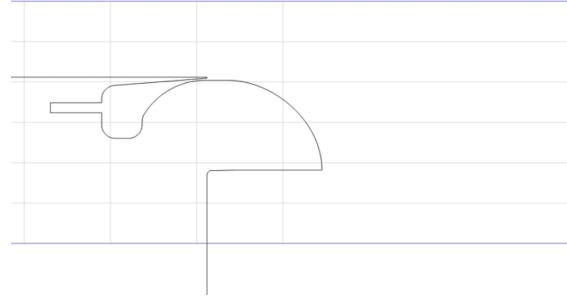
(b) Deformed Coanda jet geometry after displacement of the FFD control points. Coanda radius is 0.0283 m.

Figure 8. Coanda geometry deformation.

D.   Free-Form Deformation

A FFD strategy has become a popular geometry parameterization technique for aerodynamic shape design.[15] In FFD, an initial box encapsulating the object (rotor blade, wing, fuselage, Coanda surface, etc.) to be redesigned is parameterized as a Bézier solid. A set of control points are defined on the surface of the box, the number of which depends on the order of the chosen Bernstein polynomials. The solid box is parameterized by the following expression:

$$X(u,v,w) = \sum_{i,j,k=0}^{l,m,n} P_{i,j,k} B_i^l(u) B_j^m(v) B_k^n(w), \tag{4}$$

where u, v, $w \in [0, 1]$, and B^i is the Bernstein polynomial of order i. The Cartesian coordinates of the points on the surface of the object are then transformed into parametric coordinates within the Bézier box.

   The control points of the box become design variables, as they control the shape of the solid, and thus the shape of the surface grid inside. The box enclosing the geometry is then deformed by modifying its control points, with all the points inside the box inheriting a smooth deformation. Once the deformation has been applied, the new Cartesian coordinates of the object of interest can be recovered by simply evaluating the mapping inherent in Equation 4. After the surface has been deformed, the geometry change propagates through the mesh which is deformed by solving the linear elasticity equations.[16]

IV.   Numerical Results

   The surrogate model representing the power coefficient (C_P) can be seen in Figure 9. This surface is a low-resolution representation of the power required by the enhanced GTS model to maintain a constant speed while powering the Coanda jets. The data used to generate the surrogate model can be seen in Table 1. The generation of this response surface allows for a better understanding of the overall behavior of the vehicle under the effect of various Coanda radius and momentum coefficient (C_μ) values.

   To understand the improvements brought by the introduction of active flow control in the two-dimensional GTS model, the flow past the base GTS model has been simulated. The integrated forces and statistics have been added to Table 1 for comparison. As expected, the aerodynamic profile of this geometry is characterized by a high level of separation, vortex shedding, and a large turbulent wake that generates a low pressure region behind the vehicle. These flow features can be seen in Figures 10, 11 and 15.

   The power coefficient required for the base GTS model to maintain a constant 31.3 $\frac{m}{s}$ is 1.0235 and its vortex shedding occurs with a Strouhal number of 0.1743. Based on the results obtained from case seven, which is the lowest power consumption configuration found in this study, the drag generated by the presence of a turbulent wake in the two dimensional GTS model represents over 40% of the total drag, and the effect of using Coanda jets translates into savings of over 30% in energy consumption.
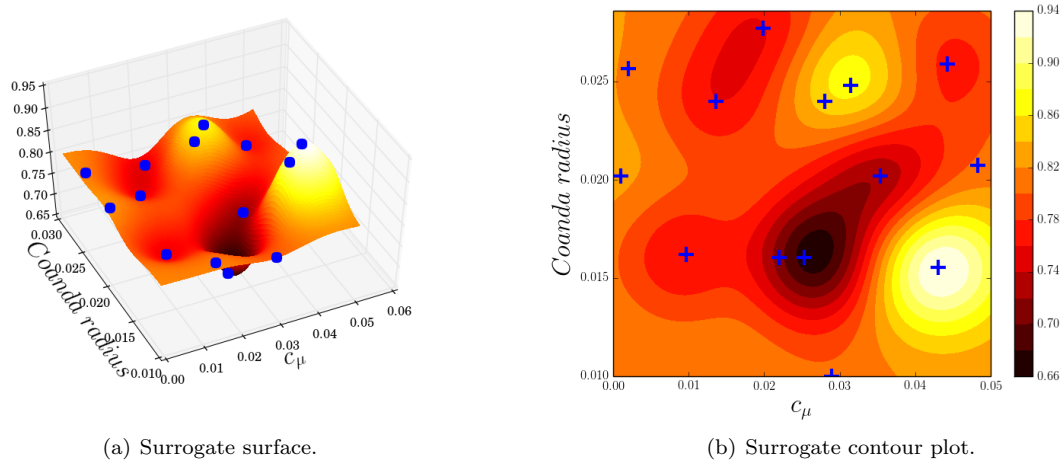
American Institute of Aeronautics and Astronautics

(a) Surrogate surface.

(b) Surrogate contour plot.

Figure 9. **Surrogate model of the power coefficient (C_P) as a function of momentum coefficient (C_μ) and Coanda radius. The blue markers are the sampling locations used to generate the response surface.**

| Case #	C_μ	Coanda radius	$\overline{C_D}$	$\widetilde{c_D}$	$\widetilde{c_{LF}}$	C_P	St
1	–	–	1.0235	$4.988e-04$	$4.342e-01$	1.0235	0.1743
2	0.0198	0.0277	0.7079	$1.289e-05$	$2.668e-02$	0.7583	0.1766
3	0.0136	0.0240	0.7322	$2.488e-05$	$4.242e-02$	0.7608	0.1743
4	0.0442	0.0259	0.6072	$1.968e-07$	$7.820e-04$	0.7744	0.0919
5	0.0096	0.0162	0.7431	$2.112e-05$	$5.951e-02$	0.7602	0.1721
6	0.0353	0.0202	0.6056	$1.979e-07$	$1.044e-03$	0.7251	0.0971
7	**0.0253**	**0.0160**	**0.5988**	**$4.193e-08$**	**$6.264e-04$**	**0.6713**	**0.1051**
8	0.0483	0.0208	0.6129	$2.284e-06$	$2.892e-03$	0.8037	0.1023
9	0.0289	0.0100	0.7162	$4.252e-07$	$2.250e-03$	0.8049	0.1013
10	0.0280	0.0240	0.7662	$2.155e-06$	$1.105e-02$	0.8506	0.1772
11	0.0430	0.0155	0.7774	$3.102e-06$	$4.815e-03$	0.9377	0.1123
12	0.0315	0.0248	0.7677	$1.371e-06$	$8.158e-03$	0.8683	0.1760
13	0.0010	0.0202	0.8243	$1.529e-04$	$1.428e-01$	0.8249	0.1694
14	0.0020	0.0257	0.8156	$1.054e-04$	$1.097e-01$	0.8172	0.1683
15	0.0220	0.0160	0.6492	$3.915e-06$	$1.766e-02$	0.7081	0.1732

Table 1. **Results for the GTS model and the enhanced GTS model injecting flow through the Coanda Jets in the trailing end at momentum coefficients ranging from 0.00 to 0.05 and Coanda radius from 0.01 to 0.0286 m. C_μ is the jet momentum coefficient, $\overline{C_D}$ is the time averaged drag coefficient, $\widetilde{c_D}$ is the drag coefficient variance, $\widetilde{c_{LF}}$ is the lateral force coefficient variance, C_P is the power coefficient, and St is the Strouhal number.**
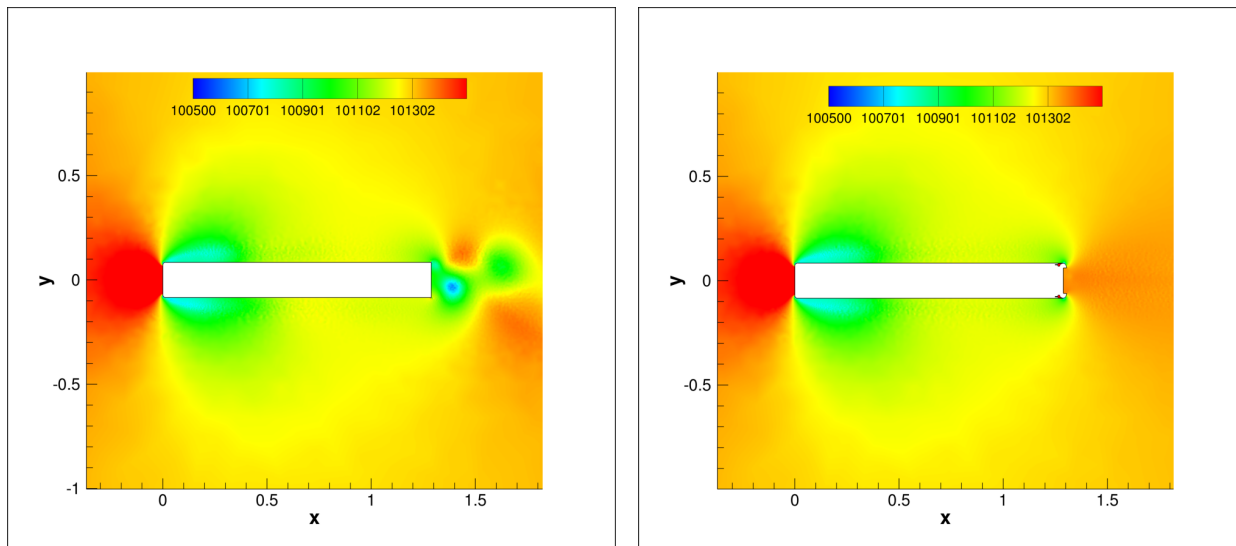
American Institute of Aeronautics and Astronautics

(a) Base GTS model.

(b) Enhanced GTS model with a Coanda radius of $0.0160\ m$ and C_μ of 0.0253. (Case 7)

Figure 10. Pressure contours of the GTS model. Pressure in Pascals.
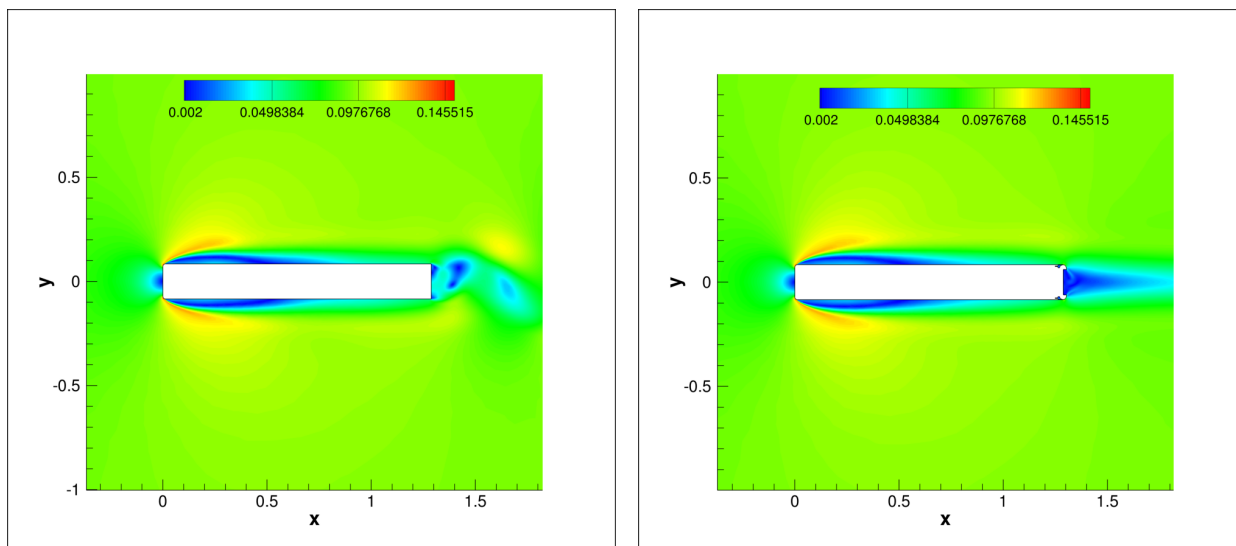
(a) Base GTS model.

(b) Enhanced GTS model with a Coanda radius of $0.0160\ m$ and C_μ of 0.0253. (Case 7)

Figure 11. Mach number contours of the GTS model.

American Institute of Aeronautics and Astronautics

The introduction of a surrogate model allows for the understanding and visualization of trends driven by the used variables, and will aid in the design of active flow control drag reduction systems. Using the surrogate as a guide, it can be seen that as the momentum coefficient increases, the incoming flow is better able to negotiate the back corners of the vehicle. This aerodynamic enhancement results in wake size reduction, a decrease in shedding frequency, and an increase in pressure inside the wake, which in turn decreases drag. Since this drag reduction is a consequence of flow being injected through Coanda jets, it is necessary to account not only for the reduction of power due to drag reduction, but also by the power required to energize the jets, relation that can be seen in Equations 1, 2 and the power coefficient from Equation 3. The power consumption behavior clearly shows that there is an ideal combination that will reduce the power requirements. Although a higher resolution of the design space is required to find the ideal Coanda jet design, the obtained response surface can be used as a guide to understand the aerodynamic changes of each configuration.
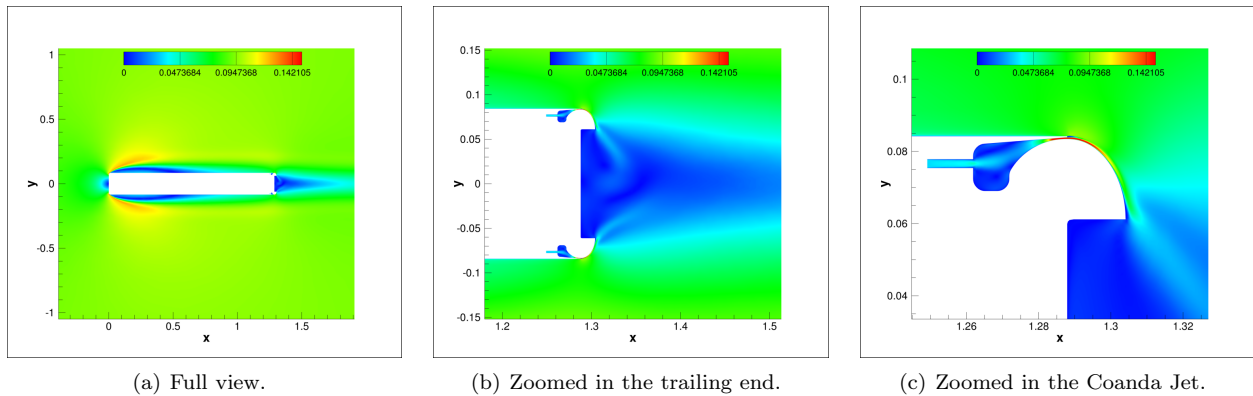

(a) Full view. (b) Zoomed in the trailing end. (c) Zoomed in the Coanda Jet.

Figure 12. Snapshot of the Enhanced GTS Mach number contour with a Coanda radius = 0.0160 m and C_μ = 0.0253. (Case 7)

The main effect that active flow control is seeking to achieve is a reduction in viscous pressure drag which can be attained by reducing the wake size. From Figure 9, is clear that as the momentum coefficient starts to increase, the vehicle power requirements drop. This phenomenon occurs due to the injection of high momentum flow into the Coanda surface, located at the trailing end of the vehicle, which allows the incoming flow to better negotiate the corners. This trend will continue until the point where the required power to energize the Coanda jets overcomes the power savings by drag reduction. An example of this condition can be seen in Figure 12, which is case seven from Table 1.
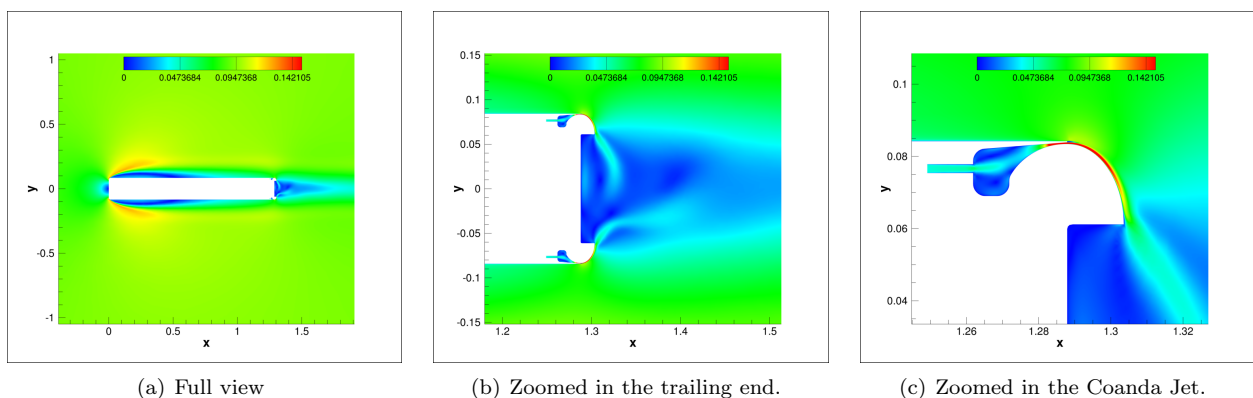

(a) Full view (b) Zoomed in the trailing end. (c) Zoomed in the Coanda Jet.

Figure 13. Snapshot of the Enhanced GTS Mach number contour with a Coanda radius = 0.0155 m and C_μ = 0.043. (Case 11)

As the momentum coefficient continues to increase, it will alter the behavior of the newly constrained wake by injecting flow that has stayed attached through the entire Coanda surface and has enough momentum to impinge on the recirculating area of the wake. The momentum injected into the wake increases the oscillation

American Institute of Aeronautics and Astronautics

frequency of this, which leads to a small increase in drag. The dominant contribution of this configuration is the excessive use of power in the Coanda jets, which leads to an overall power requirement increase. Case eleven is an example and its aerodynamic behavior can be seen in Figure 13.

A second parameter analyzed in this study is the Coanda radius, which has a highly non-linear effect on C_P. Since the flow injected follows the Coanda surface, this parameter has a direct effect on wake size. Due to the high curvature in the Coanda surface at the lower bound of the Coanda radius, the energy required to maintain the flow attached quickly overwhelms the effect of drag reduction. As the radius increases, there is an optimum combination of parameters for which the Coanda radius is ideal to maintain the jet flow attached through the entire circumference while still constraining the wake size. As the Coanda radius continues to grow, the power required to maintain the flow attached follows the same trend driving the system to a condition of high power usage where the incoming flow separates prematurely from the Coanda surface maintaining a low pressure region in the wake. Case twelve represents a relatively high C_μ configuration that lacks wake control and leads to high power requirements and the aerodynamic behavior of this configuration can be seen in Figure 14. To control the wake in a high Coanda radius configuration a higher momentum coefficient is required and, although improvements can be seen, the drag reduction is not enough to compensate for the excess energy needed to energize the jets.
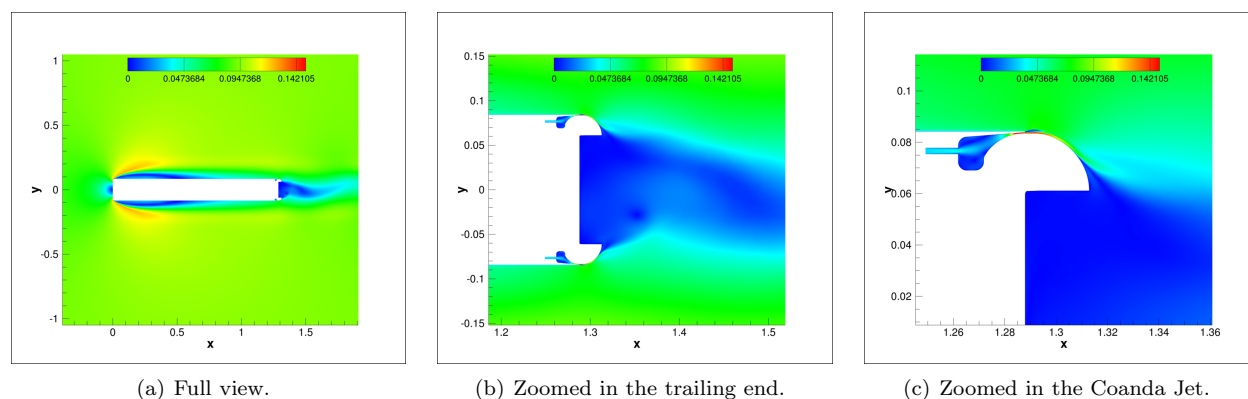

| (a) Full view. | (b) Zoomed in the trailing end. | (c) Zoomed in the Coanda Jet. |

Figure 14. Snapshot of the Enhanced GTS Mach number contour with a Coanda radius $= 0.0248\ m$ and $C_\mu = 0.0315$. (Case 12)

The lowest simulated power configuration is case seven and has been highlighted in Table 1. The combination of a Coanda radius of $0.0160\ m$ and C_μ of 0.0253 have resulted in a C_P of 0.6713 and Strouhal number of 0.1051. As expected, the flow in the front portion of both models are identical, but with the addition of the Coanda jets and the injection of flow, the wake size and vortex shedding frequency have been significantly reduced. The Mach number contours shown in Figure 11 clearly portray the reduction in the oscillatory behavior of the wake and Figure 10 clearly depicts the pressure increase in the back. To better understand the effect of the Coanda jets in the back of the GTS model, a full cycle flow representation of both the base and enhanced cases have been shown in Figure 15.

V.   Conclusion and Future Work

The flow over a two-dimensional representation of the GTS model was simulated and the effects of adding Coanda jets analyzed. To better understand the effects caused by the introduction of this type of drag reduction active flow control system, we studied the aerodynamic profile changes generated by varying the jet momentum coefficient and the Coanda radius. The effectiveness of the design was defined as a function of the power required by the vehicle to overcome the aerodynamic drag as well as to energize the jets. To minimize the required computational cost of the study, a surrogate model was generated, and the response of this has been used to understand the system's behavior.

This study has shown that as the Coanda jets start to inject air into the trailing end of the vehicle the aerodynamic drag is reduced due to an increase in the wake pressure as well as a reduction of wake size and vortex shedding frequency. As the jet strength continues to increase, the power required to energize the jets overruns the power savings due to drag reduction. As the jet strength is further increased, the fluid impinges
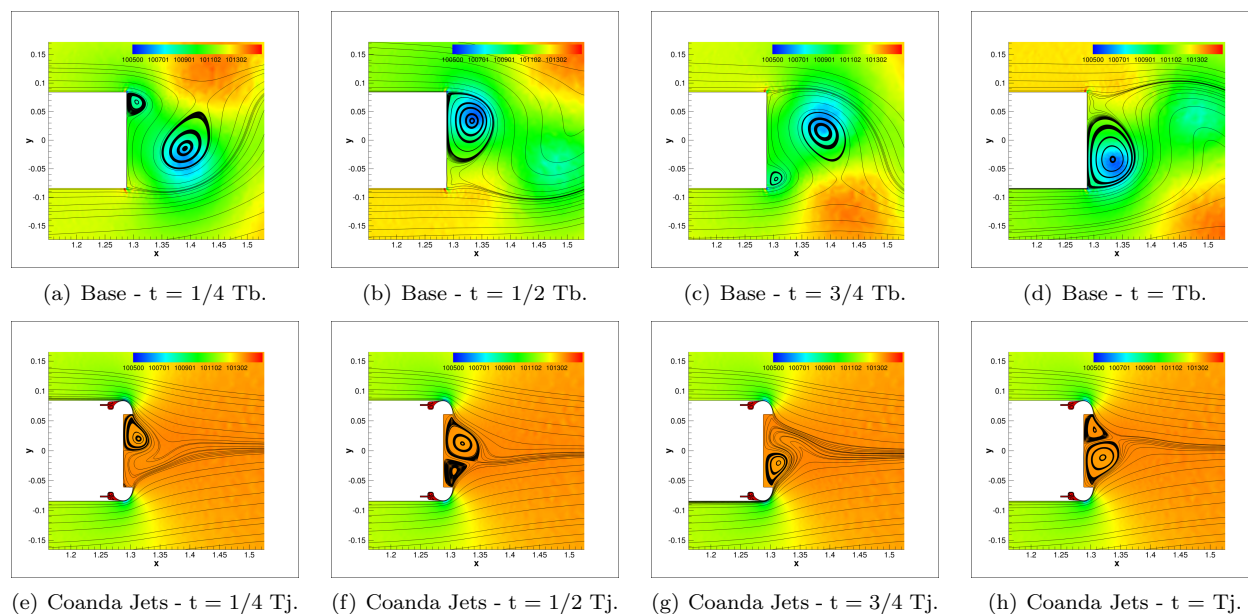
American Institute of Aeronautics and Astronautics

(a) Base - t = 1/4 Tb.   (b) Base - t = 1/2 Tb.   (c) Base - t = 3/4 Tb.   (d) Base - t = Tb.

(e) Coanda Jets - t = 1/4 Tj.   (f) Coanda Jets - t = 1/2 Tj.   (g) Coanda Jets - t = 3/4 Tj.   (h) Coanda Jets - t = Tj.

Figure 15. Pressure contours of the time history of the streamlines past the base and enhanced GTS model with a Coanda radius of 0.0160 m **and** C_μ **of** 0.0253 **(Case 7). Tb and Tj represent one shedding period for each the base case and the enhanced case respectively. Pressure in Pascals.**

on the wake introducing energy in the flow which is reflected as a slight increase in drag and vortex shedding. The prevalent effect of this configuration is the unnecessary use of power to energize the jet without the benefit of drag reduction.

In addition to the momentum coefficient, the Coanda radius has also been studied and its effects have been shown to play a significant role on the design of Coanda jets. At its lower bound, the Coanda surface exhibits a tight curvature radius which requires high momentum flow to prevent separation, which translates into a high power requirement. As the Coanda radius increases, the curvature becomes more favorable and a diminished amount of power is required for optimal performance. As the radius approaches the upper boundary, the Coanda surface length and the momentum requirements for the system to control the wake behavior increases, causing an increase in required power.

The main objective of this study was to understand the effects of the Coanda jet momentum coefficient and Coanda radius on energy consumption. Although it is well understood that the flow over the GTS model is highly three-dimensional, this study aims to gain insight into the effects each of the components forming the Coanda jet have. This information will be used to guide future studies on the three-dimensional design of active flow control drag reduction systems for heavy vehicles.

In the future, we aim to move towards the simulation of three-dimensional flows and to quantify the effect that pulsating jets and asymmetric flow injection have on the vehicle. In addition, we would like to investigate the ground-effect and its influence on the wake and the overall vehicle aerodynamics.

VI.   Acknowledgments

American Institute of Aeronautics and Astronautics

References

[1] K. Salari. DOE's effort to reduce truck aerodynamic drag through joint experiments and computations. Technical report, DOE Annual Merit Review, 2012.

[2] J. Pfeiffer and R. King. Multivariable closed-loop flow control of drag and yaw moment for a 3D bluff body. In *6th AIAA Flow Control Conference*, 2012.

[3] P. van Leeuwen. Computational analysis of base drag reduction using active flow control. Master's thesis, TU Delft, 2009.

[4] R. Englar. Advanced aerodynamic devices to improve the performance, economics, handling, and safety of heavy vehicles. *SAE Technical paper series*, 2001.

[5] D. E. Manosalvas, T. D. Economon, F. Palacios, and A. Jameson. Finding Computationally Inexpensive Methods to Model the Flow Past Heavy Vehicles and the Design of Active Flow Control Systems for Drag Reduction. *32nd AIAA Applied Aerodynamics Conference*, 2014.

[6] R. Englar. Developmetn of Pneumatic Aerodynamic Devices to Improve the Performance, Economics, and Safety of Heavy Vehicles. *SEA Technical paper series*, 2000.

[7] R. Englar, G. Jones, B. Allan, and J. Lin. 2-D Circulation Control Airfoil Benchmark Experiments Intended for CFD Code Validation. *47th AIAA Aerospace Sciences Meeting*, 2009.

[8] F. Palacios, M. Colonno, A. Aranake, A. Campos, S. Copeland, T. D. Economon, A. Lonkar, T. Taylor, and J. J. Alonso. Stanford University Unstructured (SU2): An open-source integrated computational environment for multy-physics simulation and design. *51st AIAA Aerospace Sciences Meeting*, 2013.

[9] F. Palacios, T. D. Economon, A. Aranake, S. Copeland, A. Lonkar, T. Lukaczyk, D. E. Manosalvas, K. Naik, S. Padron, B. Tracey, A. Variyar, and J. J. Alonso. Stanford University Unstructured (SU2): Open-source Analysis and Design Technology for Turbulent Flows. *52nd Aerospace Sciences Meeting*, 2014.

[10] A. Jameson, W. Schmidt, and E. Turkel. Numerical solutions of the Euler equations by finite volume methods using Runge-Kutta time-stepping schemes. *AIAA 14th Fluid and Plasma Dynamics Conference*, 1981.

[11] F. Menter. Two-equation eddy-viscosity turbulence models for engineering applications. *AIAA journal*, 32:1598–1605, 1994.

[12] A. Jameson. Time dependent calculations using multigrid, with applications to unsteady flows past airfoils and wings. *AIAA 10th Computational Fluid Dynamics Conference*, 1991.

[13] A. Forrester, A. Sobester, and A. Keane. *Engineering Design Via Surrogate Modelling: A Practical Guide.* Progress in astronautics and aeronautics. Wiley, 2008.

[14] T. Lukaczyk. *Surrogate modeling and active subspaces for efficient optimization of supersonic aircraft.* PhD thesis, Stanford University, 2015.

[15] J. A. Samareh. Aerodynamic shape optimization based on free-form deformation. *AIAA 10th Multidisciplinary Analysis and Optimization Conference*, 2004.

[16] R. P. Dwight. Robust mesh deformation using the linear elasticity equations. In *Computational Fluid Dynamics 2006*, Proceedings of the Fourth International Conference on Computational Fluid Dynamics, pages 401–406, Ghent, Belgium, July 2006. ICCFD.

American Institute of Aeronautics and Astronautics